


RESEARCH PAPER



## Thermodynamic characterization for the denatured state of bovine prion protein and the BSE Associated variant E211K

Soyoun Hwang and Eric M. Nicholson 

United States Department of Agriculture, Agricultural Research Service, National Animal Disease Center, Virus and Prion Research Unit, Ames, Iowa, USA

### ABSTRACT

Propagation of transmissible spongiform encephalopathies involves the conversion of cellular prion protein, PrP<sup>C</sup>, into a misfolded oligomeric form, PrP<sup>Sc</sup>. The most common hereditary prion disease is a genetic form of Creutzfeldt-Jakob disease in humans, in which a mutation in the prion gene results in a glutamic acid to lysine substitution at position 200 (E200K) in PrP. In cattle, the analogous amino acid substitution is found at residue 211 (E211K) and has been associated with a case of bovine spongiform encephalopathy. Here, we have compared the secondary structure of E211K to that of wild type using circular dichroism and completed a thermodynamic analysis of the folding of recombinant wild type and E211K variants of the bovine prion protein. The secondary structure of the E211K variant was essentially indistinguishable from that of wild type. The thermodynamic stability of E211K substitution showed a slight destabilization relative to the wild type consistent with results reported for recombinant human prion protein and its mutant E200K. In addition, the E211K variant exhibits a similarly compact denatured state to that of wild type based upon similar *m*-value and change in heat capacity of unfolding for the proteins. Together these results indicate that residual structure in the denatured state of bPrP is present in both the wild type protein and BSE associated variant E211K. Given this observation, as well as folding similarities reported for other disease associated variants of PrP it is worth consideration that functional aspects of PrP conformation may play a role in the misfolding process.

### ARTICLE HISTORY

Received 19 June 2018  
Revised 31 August 2018  
Accepted 3 October 2018

### KEYWORDS

TSE; prion disease; bovine prion protein; E211K; denatured state

### Introduction

Transmissible spongiform encephalopathies (TSEs) or prion diseases are a group of fatal neurodegenerative diseases that affect both humans and diverse animals. These disorders can be sporadic, inherited, or acquired by infection [1–4]. Prion diseases include scrapie in sheep and goats, bovine spongiform encephalopathy (BSE) in cattle, chronic wasting disease (CWD) in elk and deer, as well as Creutzfeldt-Jacob disease (CJD), fatal familial insomnia (FFI), Gerstmann-Sträussler-Scheinker syndrome (GSS) and kuru in humans. They are caused by the misfolding of the cellular prion protein (PrP<sup>C</sup>) into a pathogenic form (PrP<sup>Sc</sup>) in a manner such that PrP<sup>Sc</sup> can bind to and induce misfolding of new PrP<sup>C</sup> that accumulate in the CNS and some lymphoid tissues.

Bovine PrP<sup>C</sup> (bPrP) is a glycoprotein of 217 amino acid residues and anchored to the cell membrane via a glycosylphosphatidylinositol (GPI) moiety at its C-terminal and there are two N-glycosylation sites allowing posttranslational modification at Asn181 and

Asn197 and a single disulfide bond between Cys179 and Cys214 connecting the longer two helices. The three-dimensional NMR structure of recombinant bPrP was determined by Wüthrich and his colleagues [5]. The NMR structure showed that the folded C-terminal region (121–230) contains three  $\alpha$ -helices and a short antiparallel  $\beta$ -sheet whereas the N-terminal region is highly flexible and disordered. This result is consistent with the structure of recombinant human prion protein (Figure 1). Recombinant proteins, however, do not include the post-translational modifications of PrP<sup>C</sup>. Wüthrich and his colleagues compared the detailed structure and stability between recombinant bPrP and cellular prion protein isolated from healthy calf brains using circular dichroism (CD) and NMR spectroscopy to determine applicability of recombinant PrP studies to the true biological process concluding that three-dimensional structure and thermal stability of the natural glycoprotein isolated from a calf and the recombinant proteins are essentially identical [6].

The denatured state of a protein is an ensemble of interconverting conformations [7]. Denatured proteins

**CONTACT** Eric M. Nicholson  [eric.nicholson@ars.usda.gov](mailto:eric.nicholson@ars.usda.gov); [eric.m.nicholson@gmail.com](mailto:eric.m.nicholson@gmail.com)  United States Department of Agriculture, Agricultural Research Service, National Animal Disease Center, Virus and Prion Research Unit, Ames, Iowa, USA

© 2018 The Author(s). Published by Informa UK Limited, trading as Taylor & Francis Group.  
This is an Open Access article distributed under the terms of the Creative Commons Attribution-NonCommercial-NoDerivatives License (<http://creativecommons.org/licenses/by-nc-nd/4.0/>), which permits non-commercial re-use, distribution, and reproduction in any medium, provided the original work is properly cited, and is not altered, transformed, or built upon in any way.

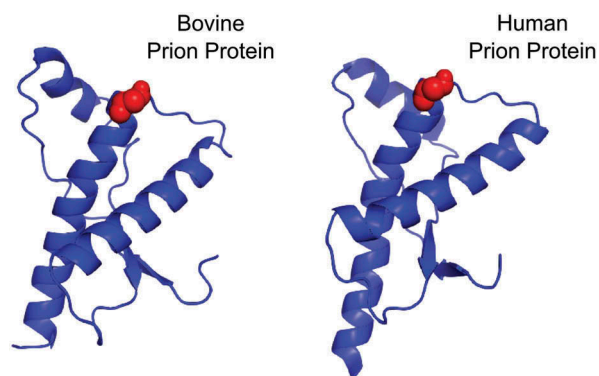


**Figure 1.** Ribbon diagram of the bovine and human prion protein structure showing the location of the amino acid substitution. The figure was generated using the PYMOL (open source version, Schrödinger LLC, Portland, OR) and NMR solution structure of bovine and human PrP. (PDB code: 1DX1 and 1QM1). The red colored label indicates the glutamic acid residue at 211 (bovine) and 200 (human).

contain considerable amounts of native and non-native structure, both of which may provide information about early folding events [8–10]. Spectroscopic techniques such as nuclear magnetic resonance (NMR) allow the observation of residual structure in the denatured state of a number of proteins [11,12]. The existence of residual structure in specific regions of the denatured state showed a good correlation with the regions found to fold early by protein engineering methods [10] indicating that residual denatured state structure can play an important role in the folding initiation. Theoretical simulations further support the importance of residual structure in nucleation of the folding process [13,14]. Insight into denatured state conformation may also be obtained using thermodynamic approaches. Myers et al. established the strong correlation between  $m$  values, the dependence of the free energy of unfolding on denaturant concentration, and the change in a surface area of protein exposed to solvent upon unfolding ( $\Delta ASA$ ), and between  $\Delta ASA$  and  $\Delta C_p$ , change of molar heat capacity at constant pressure, for a large set of proteins [15]. Robertson et al. reported similar results with 49 different proteins [16], indicating that  $\Delta C_p$  is proportional to the number of residues further supporting  $\Delta ASA$  to  $\Delta C_p$  correlation.

In 2006, a case of genetically associated H-type BSE was diagnosed in the U.S. The animal had a polymorphism that resulted in a glutamic acid at residue 211 to lysine substitution, a change analogous to the human E200K mutation that is the most common form of genetic Creutzfeldt-Jakob disease [17]. As can be seen in Figure 1, the glutamic acid at position 211 is located on the protein surface like glutamic acid at location 200 of

recombinant human prion protein. The NMR structure of the E200K variant of human prion protein was calculated and determined to be nearly identical to that of wild type human prion protein except for minor differences in flexible regions [18]. In the present study, to assess whether E211K protein has different residual structures in the denatured state compared to bPrP wild type, we determine urea  $m$ -values and the change in heat capacity upon unfolding of the proteins.

## Results

### Effect of E211K mutation on secondary structure

- Circular dichroism spectroscopy was used to evaluate changes in the structure induced by the point mutation from glutamic acid to lysine at residue 211. Characteristic minimum at 208 nm and 222 nm in far-UV CD spectra demonstrated that wild-type protein and the mutant had predominantly  $\alpha$ -helical structure indicating that mutation did not result in major conformational change. The CD spectra of E211K protein at pH 7.0 was similar to that of wild-type shown in Figure 2, indicating only minimal structural changes due to the E211K substitution.

### Effect of E211K mutation on the thermodynamic properties

**Chemical denaturation-** The effect of mutation on the global free energy of unfolding ( $\Delta G_{unf}$ ) of recombinant bPrP was probed by equilibrium urea unfolding. At pH 7, the unfolding of both the wild-type and E211K protein was assumed as a two-state folding mechanism shown in Figures 3 and 4, and under that

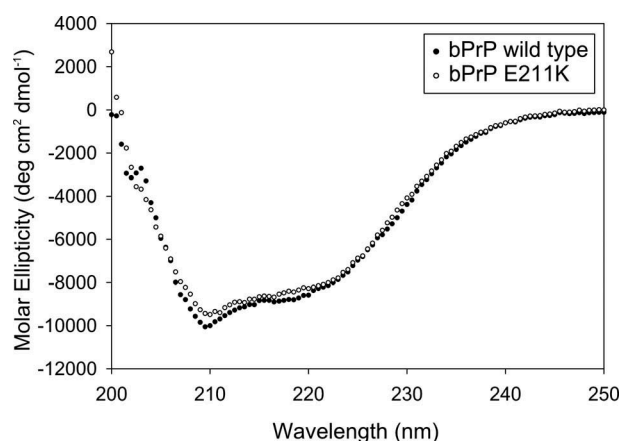


**Figure 2.** Far-UV circular dichroism spectra of bPrP (25–241) variants. Circular dichroism spectra recorded in 10 mM phosphate buffer, pH 7.0. Closed circle indicates bPrP wild type and open circle indicates E211K variant.

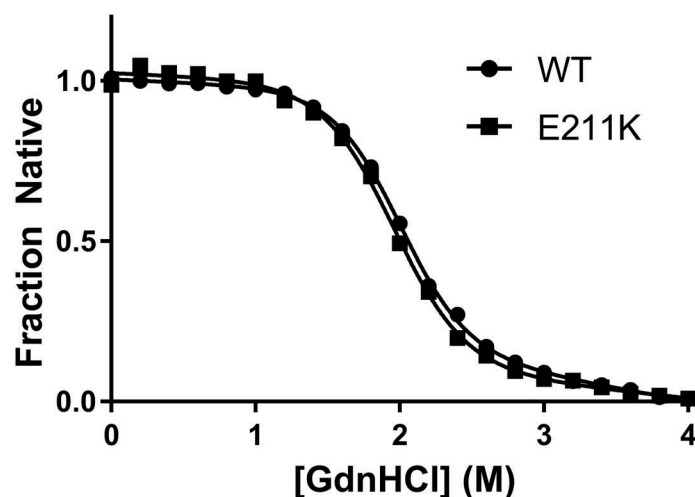


**Figure 3.** Unfolding of bPrP wild-type and E211K variant in guanidine hydrochloride at pH 7.0 measured at 25 °C. Closed circles represent the wild type protein, and closed squares represent the E211K mutant. The data for the E211K variant does not show any significant difference to that of the wild-type protein.

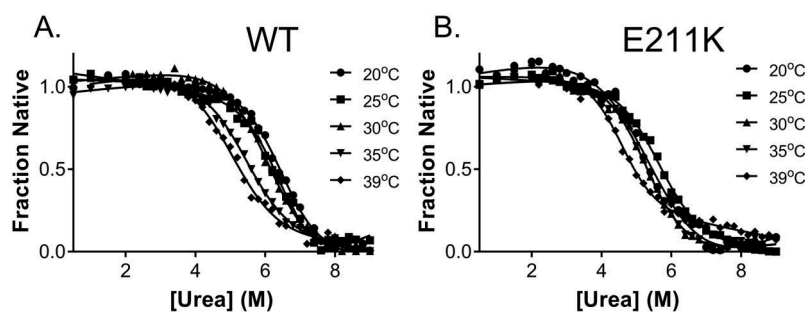


**Figure 4.** Representative urea-unfolding curves for bPrP wild type (A) and E211K variant (B) measured at 20 °C, 25 °C, 30 °C, 35 °C, and 39 °C. The curve through the points depicts the best fit to the data as described in Materials and Methods using Equation 1 providing the  $C_{mid}$  and  $m$ -values for bPrP wild type and E211K proteins at each indicated temperature. Results of the data are summarized in Table 1.

**Table 1.** Parameters summarizing the urea denaturation of recombinant bPrP wild type (25–241) and E211K variant in 10 mM potassium phosphate buffer, pH 7.0, at the indicated temperatures.

Temperature (°C)	<sup>a</sup> $m$ (kcal/mol·M)		<sup>b</sup> $C_{mid}$ (M)		<sup>c</sup> $\Delta G_{(H_2O)}$ (kcal/mol)	
	WT	E211K	WT	E211K	WT	E211K
20	1.06 ± 0.04	1.05 ± 0.02	6.48 ± 0.02	5.33 ± 0.28	6.87	5.6
25	1.05 ± 0.11	0.94 ± 0.05	6.55 ± 0.03	5.60 ± 0.06	6.88	5.26
30	0.99 ± 0.07	1.02 ± 0.09	6.04 ± 0.03	5.33 ± 0.09	5.98	5.44
35	1.04 ± 0.09	1.14 ± 0.2	5.51 ± 0.12	4.92 ± 0.24	5.73	5.61
39	1.23 ± 0.04	1.11 ± 0.11	5.10 ± 0.01	4.37 ± 0.2	6.27	4.85

All values reported as the mean ± standard deviation.

<sup>a</sup> <sup>b</sup> Best fit parameters to Equation (1) and the confidence intervals as one standard deviation <sup>c</sup>  $\Delta G_{(H_2O)} = m * C_{mid}$ .

<sup>a</sup> $m$ : The slope of plots of  $\Delta G$  vs. [denaturant]

<sup>b</sup> $C_{mid}$ : Midpoint of the unfolding curve

<sup>c</sup> $\Delta G_{(H_2O)}$  = the intercept of plots of  $\Delta G$  vs [Urea] at 0 M urea

Data presented with ± values indicates standard deviations (SD).

assumption, the  $\Delta G$ , unfolding free energy was determined as a function of denaturant concentration.  $\Delta G$  is linearly related to the concentration of denaturant, urea or guanidine hydrochloride, as:

$$\Delta G = \Delta G_{(H_2O)} - m[\text{denaturant}] \quad (1)$$

where  $\Delta G_{H_2O}$  is the free energy of unfolding in the absence of denaturant, and  $m$  is the denaturant dependence to stability [19]. Thermodynamic stability of bPrP proteins was probed by equilibrium unfolding in GdnHCl at 25 °C. As can be seen from GdnHCl unfolding curves (Figure 3), the difference between the wild

type bPrP and E211K variant is negligible. Considering the charge differential of the E211K variant and the strong ionic screening effect of GdnHCl, urea was subsequently chosen and used for this study. Urea denaturation curves, were determined at temperatures from 20 to 39 °C to evaluate the temperature effect on the thermodynamic parameters. The results of the urea unfolding curves at different temperatures are summarized in Table 1. Overall, the  $\Delta G_{H_2O}$  value of unfolding for wild-type protein was higher than that of E211K protein. Denaturant *m* value for wild type was similar to the *m* value for E211K protein indicating that the wild-type protein has a similar change in solvent accessible area ( $\Delta ASA$ ) upon unfolding.

**Thermal denaturation-** In order to evaluate  $\Delta C_p$ , as part of a thermodynamic investigation of the denatured state, thermal denaturation curves were measured for the wild-type and E211K proteins. The thermal denaturation curves in the presence of urea ranging from 0 M to 3.5 M of wild-type and E211K are shown in Figure 5 and the results of the fit to the data are summarized in Table 2. In this study, we have adopted the nomenclature of Schellman where the subscript ‘g’ indicates the parameter at a reference temperature,  $T_g$ , where  $\Delta G = 0$  [20]. Thermal denaturation of

recombinant proteins, wild-type and E211K, were reversible with 90 % of the original signal at 222 nm after cooling. At successively higher concentrations of urea, the  $T_g$  of both wild-type and E211K PrP decreased as expected (see Figure 5 and Table 2). These experiments were analyzed as described in the methods section to determine the midpoint of the thermal denaturation curve,  $T_g$  and the van’t Hoff enthalpy change,  $\Delta H_{g,shc}$  at each denaturant concentration. In the absence of denaturant the  $T_g$  for wild-type was  $70.6 \pm 0.5$  °C and for E211K protein was  $67.8 \pm 0.5$  °C. Overall, both urea and thermal denaturation data suggests that E211K variant has a slightly lower stability than the wild-type, an observation that is in agreement with that previously reported for human wild-type and E200K prion proteins.

The change heat capacity at constant pressure ( $\Delta C_p$ ) values were determined for both wild-type and E211K PrP. In order to determine the heat capacity change for folding, the Kirchhoff equation was used.

$$\frac{d(\Delta H_g)}{d(T_g)} = \Delta C_p \quad (2)$$

The plot of  $\Delta H_g$  as a function of  $T_g$  is shown in Figure 6 for the wild-type and E211K proteins. The

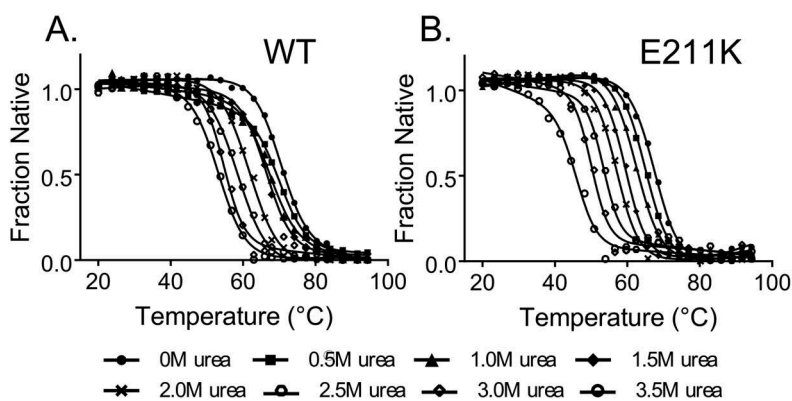


**Figure 5.** Representative thermal unfolding curves for bPrP wild type (A) and E211K variant (B) in 10 mM phosphate buffer, pH 7.0. The curve through the points is the best fit of the data to Equation (2) in the Materials and Methods. The results of the data are summarized in Table 2.

**Table 2.** Parameters summarizing thermal denaturation in the presence of urea of recombinant bPrP wild type (25–241) and E211K variant.

[Urea] (M)	Wild type		E211K	
	$T_g$ (°C)	$\Delta H_g$ (kcal/mol)	$T_g$ (°C)	$\Delta H_g$ (kcal/mol)
0	$70.6 \pm 0.5$	$59.4 \pm 0.5$	$67.8 \pm 0.5$	$67.5 \pm 3.0$
0.5	$68.6 \pm 0.5$	$61.1 \pm 1.0$	$65.1 \pm 0.5$	$64.6 \pm 2.5$
1.0	$66.7 \pm 0.5$	$61.2 \pm 6.0$	$62.6 \pm 0.5$	$58.1 \pm 0.4$
1.5	$64.4 \pm 0.5$	$61.0 \pm 1.0$	$61.0 \pm 0.5$	$52.0 \pm 2.0$
2.0	$62.4 \pm 0.5$	$50.6 \pm 2.0$	$58.0 \pm 0.5$	$54.7 \pm 1.5$
2.5	$59.8 \pm 0.5$	$48.6 \pm 6.0$	$55.5 \pm 0.5$	$49.7 \pm 2.0$
3.0	$56.4 \pm 0.5$	$48.9 \pm 1.0$	$51.4 \pm 0.5$	$47.7 \pm 1.7$
3.5	$53.6 \pm 0.5$	$43.1 \pm 2.0$	$49.5 \pm 0.5$	$45.2 \pm 5.0$

All values are the best fit parameters to Equation (2) with confidence intervals as one standard deviation.

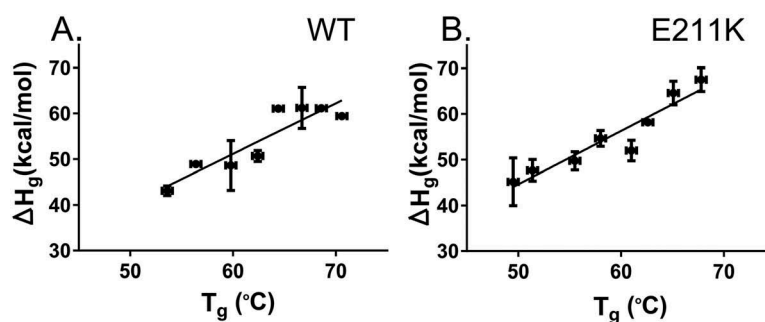


**Figure 6.**  $\Delta H_g$  plotted as a function of  $T_g$  for the wild type and E211K bPrP variants, using values indicated in Table 2 for bPrP wild type (A) and E211K mutant (B). The lines are least-squares fit to Equation (4). The  $\Delta C_p$  of both proteins was similar for wild type and E211K bPrP.

values are given in Table 2. The  $\Delta C_p$  for wild-type was determined to be  $1.02 \text{ kcal mol}^{-1}\text{K}^{-1}$  and  $1.03 \text{ kcal mol}^{-1}\text{K}^{-1}$  for E211K mutant. The  $\Delta C_p$  of both proteins was similar for bPrP wild-type and E211K variants.

## Discussion and conclusions

In this study, the thermodynamics of unfolding of recombinant bovine prion protein was studied with its disease associated, hereditary variant (E211K) using chemical and thermal denaturation to determine if differences between the two variants of the prion protein manifest in a thermodynamically detectable manner. Early efforts in the understanding of genetic prion disease found little evidence to support a change in the global stability as a means to explain enhanced misfolding in the disease associated variants [21]. Subsequent study then focused on the identification of folding intermediates using a variety of approaches that all showed that the C-terminal portion of the prion protein folded more rapidly [22,23]. Investigation into pre-oligomer structures also showed the presence of an acid-induced molten globule state where the C-terminal region remained folded but under physiologic conditions an equilibrium intermediate is not detected [24]. Native state hydrogen exchange experiments monitored by NMR indicated that the C-terminal region was more stable than the N-terminal region [25]. Interestingly, this study also showed protection against hydrogen exchange above that expected based on the global stability of the protein. This observation is consistent with either structure in the denatured state or the presence of an undetected intermediate. An undetected intermediate in the urea denaturation would result in an underestimation of the global stability. However, efforts to detect such an intermediate found no evidence [24] leaving structure in the denatured state the most suitable

explanation. To determine if residual structure in the denatured state of bovine prion protein could explain the enhanced disease of bPrP E211K variants, we investigated the thermodynamic parameters describing the unfolding of bPrP wild type and E211K proteins with the first observation being that the E211K mutation gave a total decrease in stability of  $1.62 \text{ kcal mol}^{-1}$ , and a melting temperature  $2.8 \text{ }^\circ\text{C}$  lower than the wild-type protein. However, as was concluded for the human E200K variant [21], the small reduction in stability is insufficient to explain an enhanced disease phenotype in the E211K bPrP. Given this result and previously mentioned observation that PrP may contain significant residual structure in the denatured state we elected to focus further on thermodynamic parameters that report more specifically on the denatured state.

The basis for our approach originates from the established correlation between both the  $\Delta C_p$  and  $m$ -value and the change in solvent accessible surface area upon unfolding [15]. Myers et al. showed the presence of correlations between,  $\Delta\text{ASA}$  and number of residues,  $m$  and  $\Delta\text{ASA}$ , and also between  $\Delta C_p$  and  $\Delta\text{ASA}$  concluding that there is a significant linear correlation in all cases. For mature bPrP (25–241), the predicted value for the  $m$  value is  $2.49 \text{ kcal mol}^{-1}\text{M}^{-1}$  and  $3.41 \text{ kcal mol}^{-1}\text{K}^{-1}$  for  $\Delta C_p$ , both of which are considerably higher than the measured values of  $m = 1.05 \text{ kcal mol}^{-1}\text{M}^{-1}$  and  $\Delta C_p = 1.02 \text{ kcal mol}^{-1}\text{K}^{-1}$  for wild type bPrP (Table 3). The  $m$  value and  $\Delta C_p$ , for bPrP (25–241) are less than half that predicted for a protein of similar size. Given the extensive unfolded region at the N-terminus of bPrP [5] we estimated the  $m$  value and  $\Delta C_p$  based upon the sequence length of the structured region only and obtained values of  $1.39 \text{ kcal mol}^{-1}\text{M}^{-1}$  and  $1.502 \text{ kcal mol}^{-1}\text{K}^{-1}$  for the  $m$  value and  $\Delta C_p$  respectively. This improved but did not fully align the agreement between estimated and measured values with measured values still lower than predicted based

**Table 3.** Predicted solvent accessible area and *m* values for mature and structured region of bPrP.

	Predicted $\Delta$ ASA ( $\text{\AA}^2$ )	Predicted <i>m</i> (kcal/mol-M)	Predicted $\Delta C_p$ (kcal/mol-K)
mature bPrP (25–241)	19,274	2.49	3.41
structured bPrP (122–230)	9230	1.39	1.50

upon the size of the protein. As an experimental justification for calculating a predicted *m* value based only on the structured region is the observation that the *m* values for both mature length mouse PrP (23–231) and a variant with the unstructured N-terminal region removed (121–231) are in agreement [26].

In addition to comparing the measured and calculated *m* value and  $\Delta C_p$  of wild type bPrP, the *m* values and  $\Delta C_p$  of E211K bPrP were measured and compared to the measured parameters for wild type bPrP and found to be within the error of the measurement. Similar denaturant *m* values and  $\Delta C_p$  between wild type and E211K protein is indicative of similar  $\Delta$ ASA. Given the similarity of the native state measured by NMR [18] and an equivalent  $\Delta$ ASA upon unfolding, the two proteins must also have similar denatured states. Lacking native state differences, denatured state differences or substantial differences in the thermodynamic parameters describing stability, the substitution of lysine for glutamic acid results in genetic prion disease through mechanisms not exclusively related to the folding and stability of PrP, with some functional aspect such as metal ion binding also influencing the misfolding process. Suggestions have been made that this may occur due to differences in the oxidative stress response [27] or levels of expression for the disease associated variant [28], data available to date does not support this [29] in cattle.

Thermodynamic analysis of protein folding as utilized in this study is inherently limited with regard to the inability to define the folding mechanism, and it is sometimes considered to be a limited technique suitable for little more than determining the difference in the free energy or change in enthalpy between the native and denatured states. As utilized in this study, additional analysis of the thermodynamic parameters defining the equilibrium folding and comparison to values in the literature inform us with regard to the denatured state of wild-type and E211K bovine rPrP. While we can say with confidence that the compactness of the denatured states of these two proteins are more compact than typical and that they are in reasonable agreement with each other. However, we cannot claim that the compact denatured states are structurally equivalent or that they have the same numbers of native contacts allowing for the possibility that the activation barrier for folding may differ for wild type and E211K bovine rPrP.

In summary, our results indicate that the *m* value and  $\Delta C_p$  are somewhat lower than expected for a protein with structured region of comparable size to bPrP, a result consistent with residual structure in the denatured state or undetected intermediate. However, lacking a difference in either *m* value or  $\Delta C_p$  between the wild type and E211K variants implies the enhanced disease associated with the E211K variant is not due to differences in the denatured state.

## Materials and methods

**Protein Production-** The expression and purification of bPrP (25–241) was performed using Method I as described in Vrentas et al [30]. Briefly, *E. coli* strain BL21 ( $\lambda$ DE3) containing either the wild-type bovine prion gene or the E211K variant were cultured in separate flasks of LB medium (5 ml) supplemented with kanamycin (50  $\mu$ g/ml). The cells were grown at 37 °C with shaking at 250 rpm. After 16 hours, 2 ml of each culture was then transferred to fresh 1 L of LB medium containing the same concentrations of antibiotics. The cultures were grown at 37 °C, induced, and harvested by centrifugation, and the cell pellet was suspended and analyzed. Prepared inclusion bodies were mixed with 60 – 80 ml buffer including 6 M guanidine-HCl, 10 mM Tris-HCl (pH 8), 0.1 M  $\text{Na}_2\text{HPO}_4$ , 0.5 % Triton X-100 and incubated at room temperature for 1 h before overnight incubation at 4 °C on a platform rocker. Wild-type and E211K were isolated using Ni-NTA (Nickel) resin (Clontech, #635,502) and washed and eluted as described. All eluted pooled fractions were diluted to a final protein concentration of 0.5 mg/ml and dialyzed overnight into IMAC buffer containing 8 M urea, 0.1 M  $\text{Na}_2\text{HPO}_4$ , and 10 mM Tris-HCl, pH adjusted to 8 and the second dialysis was performed overnight into 10 mM potassium phosphate buffer, pH adjusted to 7. Concentration of pooled protein eluent was determined by UV absorbance at 280 nm using an extinction coefficient of 63,495  $\text{M}^{-1}\text{cm}^{-1}$  as calculated for wild-type and E211K.

**Secondary Structure evaluation by Far-UV Circular Dichroism spectroscopy-** Far UV circular dichroism (CD) spectra were recorded on a Jasco J-815 spectropolarimeter equipped with a temperature

control. All spectra were recorded by averaging three scans in the 200 – 260 nm range at a scan rate of 10 nm/min. Spectra were acquired at a protein concentration of 2–3  $\mu\text{M}$  using 1 cm path length cell.

**Chemical denaturation-** Circular dichroism at 222 nm was used to monitor the equilibrium unfolding transition. Samples in the presence of urea were incubated for 16 h at room temperature to equilibrate prior to data collection. For the urea denaturation curves at ranged from 20 to 39  $^{\circ}\text{C}$  were performed and the 10 M urea solutions were prepared fresh daily in 10 mM potassium phosphate buffer at pH 7.0. For urea unfolding curves, data were analyzed by using a two state transition model as described previously [31]. To determine the concentration of denaturant at the midpoint of the unfolding curve ( $C_{\text{mid}}$ ) and  $m$ , slope of free energy as a function of denaturant concentration for each urea denaturation curve, CD signal was plotted as a function of urea and fit using equation below,

$$Y = \frac{[(\text{No} + (\text{aN} * [\text{urea}])) + ((\text{Do} + (\text{aD} * [\text{urea}])) * \exp\left[\left(\frac{m}{RT}\right) * ([\text{urea}] - C_{\text{mid}})\right])]}{1 + \exp\left[\left(\frac{m}{RT}\right) * ([\text{urea}] - C_{\text{mid}})\right]} \quad (3)$$

where No is the intercept of native baseline, aN is the slope of the native baseline, [urea] is the molar concentration of urea, Do is the intercept of denatured protein, and aD is the slope of the denatured baseline.

The concentration of the urea stock solution was determined by refractive index measurement [32]. Reversibility of denaturant induced unfolding was confirmed by the return of appropriate CD signal at 222 nm after the dilution of a sample from urea unfolding conditions to refolding conditions.

**Thermal denaturation-** Thermal denaturation curves were monitored by CD at 222 nm with a protein concentration of 2–3  $\mu\text{M}$  over the temperature range of 20 – 95  $^{\circ}\text{C}$ . The heating rate in all experiments was 1  $^{\circ}\text{C}/\text{min}$ . The thermal denaturation curves, CD signals were plotted as a function of temperature and fit to determine  $T_g$  and the van't Hoff enthalpy of denaturation ( $\Delta H_g$ ) with equation below [33].

$$Y = \frac{[(\text{No} + (\text{aN} * T)) + (\text{Do} + (\text{aD} * T) \left[ \exp\left[\frac{\Delta H_g}{R} * \left(\frac{1}{T_g} - \frac{1}{T}\right)\right]\right])]}{1 + \exp\left[\frac{\Delta H_g}{R} * \left(\frac{1}{T_g} - \frac{1}{T}\right)\right]} \quad (4)$$

No is the intercept of native baseline, aN is the slope of the native baseline, Do is the intercept of

denatured protein, aD is the slope of the denatured baseline, T is the temperature in Kelvin, R is the gas constant, and  $T_g$  is the temperature at the midpoint of the transition and  $\Delta H_g$  is the enthalpy of unfolding at this temperature. Using urea to perturb the  $T_g$  provided  $\Delta H_g$  at different temperatures and  $\Delta C_p$  was obtained from the linear temperature dependence of van't Hoff enthalpy at using different urea concentration [34]. Curves were fit with the indicated relationships in either GraphPad or SigmaPlot (Systat Software, San Jose, CA) providing the thermodynamic parameters,  $T_g$ ,  $\Delta H_g$ , and  $\Delta C_p$ . Thermal denaturation in the absence of urea was confirmed to be reversible by heating into the transition region of the unfolding curve and returning to 20  $^{\circ}\text{C}$  with no discernable loss in secondary structure. Samples heated in urea exhibited substantial reduction in a reversibility, presumably due to chemical modification by urea break down products.

## Disclaimer

Mention of trade names or commercial products in this publication is solely for the purpose of providing specific information and does not imply recommendation or endorsement by the U.S. Department of Agriculture. USDA is an equal opportunity provider and employer.

## Acknowledgments

The authors thank Semakaleng Lebepe-Mazur for providing technical support to this project.

## Disclosure statement

No potential conflict of interest was reported by the authors.

## Funding

This research was funded in its entirety by congressionally appropriated funds to the United States Department of Agriculture, Agricultural Research Service. The funder of the work did not influence study design, data collection and analysis, decision to publish, and preparation of the manuscript.

## Author contribution

Conceived and designed the experiments: EMN SH. Performed the experiments: SH. Analyzed the data: EMN SH. Wrote the paper: EMN SH.;

## ORCID

Eric M. Nicholson  <http://orcid.org/0000-0002-2217-0161>

## References

- [1] Prusiner SB. Prions. *Proc Natl Acad Sci USA*. 1998;95:13363–13383.
- [2] Collinge J. Prion diseases of humans and animals: their causes and molecular basis. *Annu Rev Neurosci*. 2001;24:519–550.
- [3] Caughey B, Chesebro B. Transmissible spongiform encephalopathies and prion protein interconversions. *Adv Virus Res*. 2001;56:277–311.
- [4] Weissmann C. The ninth datta lecture. molecular biology of transmissible spongiform encephalopathies. *FEBS Lett*. 1996;389:3–11.
- [5] Lopez Garcia F, Zahn R, Riek R, et al. NMR structure of the bovine prion protein. *Proc Natl Acad Sci USA*. 2000;97:8334–8339.
- [6] Hornemann S, Schorn C, Wuthrich K. NMR structure of the bovine prion protein isolated from healthy calf brains. *EMBO Rep*. 2004;5:1159–1164.
- [7] Cho JH, Raleigh DP. Experimental characterization of the denatured state ensemble of proteins. *Methods Mol Biol*. 2009;490:339–351.
- [8] Yao J, Chung J, Eliezer D, et al. NMR structural and dynamic characterization of the acid-unfolded state of apomyoglobin provides insights into the early events in protein folding. *Biochemistry*. 2001;40:3561–3571.
- [9] Wright PE, Dyson HJ, Lerner RA. Conformation of peptide fragments of proteins in aqueous solution: implications for initiation of protein folding. *Biochemistry*. 1988;27:7167–7175.
- [10] Freund SM, Wong KB, Fersht AR. Initiation sites of protein folding by NMR analysis. *Proc Natl Acad Sci U S A*. 1996;93:10600–10603.
- [11] Blanco FJ, Serrano L, Forman-Kay JD. High populations of non-native structures in the denatured state are compatible with the formation of the native folded state. *J Mol Biol*. 1998;284:1153–1164.
- [12] Kortemme T, Kelly MJ, Kay LE, et al. Similarities between the spectrin SH3 domain denatured state and its folding transition state. *J Mol Biol*. 2000;297:1217–1229.
- [13] Radford SE, Dobson CM. From computer simulations to human disease: emerging themes in protein folding. *Cell*. 1999;97:291–298.
- [14] Thirumalai D, Klimov DK. Fishing for folding nuclei in lattice models and proteins. *Fold Des*. 1998;3: R112–R118. discussion R107.
- [15] Myers JK, Pace CN, Scholtz JM. Denaturant  $m$  values and heat capacity changes: relation to changes in accessible surface areas of protein unfolding. *Protein Sci*. 1995;4:2138–2148.
- [16] Robertson AD, Murphy KP. Protein structure and the energetics of protein stability. *Chem Rev*. 1997;97:1251–1268.
- [17] Hsiao K, Meiner Z, Kahana E, et al. Mutation of the prion protein in Libyan Jews with Creutzfeldt-Jakob disease. *N Engl J Med*. 1991;324:1091–1097.
- [18] Zhang Y, Swietnicki W, Zagorski MG, et al. Solution structure of the E200K variant of human prion protein. Implications for the mechanism of pathogenesis in familial prion diseases. *J Biol Chem*. 2000;275:33650–33654.
- [19] Greene RF Jr., Pace CN. Urea and guanidine hydrochloride denaturation of ribonuclease, lysozyme, alpha-chymotrypsin, and beta-lactoglobulin. *J Biol Chem*. 1974;249:5388–5393.
- [20] Bechtel WJ, Schellman JA. Protein stability curves. *Biopolymers*. 1987;26:1859–1877.
- [21] Swietnicki W, Petersen RB, Gambetti P, et al. Familial mutations and the thermodynamic stability of the recombinant human prion protein. *J Biol Chem*. 1998;273:31048–31052.
- [22] Apetri AC, Maki K, Roder H, et al. Early intermediate in human prion protein folding as evidenced by ultra-rapid mixing experiments. *J Am Chem Soc*. 2006;128:11673–11678.
- [23] Honda RP, Xu M, Yamaguchi KI, et al. A native-like intermediate serves as a branching point between the folding and aggregation pathways of the mouse prion protein. *Structure*. 2015;23:1735–1742.
- [24] Honda RP, Yamaguchi K, Kuwata K. Acid-induced molten globule state of a prion protein: crucial role of Strand 1-Helix 1-Strand 2 segment. *J Biol Chem*. 2014;289:30355–30363.
- [25] Nicholson EM, Mo H, Prusiner SB, et al. Differences between the prion protein and its homolog Doppel: a partially structured state with implications for scrapie formation. *J Mol Biol*. 2002;316:807–815.
- [26] Moulick R, Udgaonkar JB. Thermodynamic characterization of the unfolding of the prion protein. *Biophys J*. 2014;106:410–420.
- [27] Canello T, Friedman-Levi Y, Mizrahi M, et al. Copper is toxic to PrP-ablated mice and exacerbates disease in a mouse model of E200K genetic prion disease. *Neurobiol Dis*. 2012;45:1010–1017.
- [28] Rosenmann H, Halimi M, Kahana I, et al. Differential allelic expression of PrP mRNA in carriers of the E200K mutation. *Neurology*. 1997;49:851–856.
- [29] Vrentas CE, Greenlee JJ, Foster GH, et al. Effects of a naturally occurring amino acid substitution in bovine PrP: a model for inherited prion disease in a natural host species. *BMC Res Notes*. 2017;10:759.
- [30] Vrentas CE, Onstot S, Nicholson EM. A comparative analysis of rapid methods for purification and refolding of recombinant bovine prion protein. *Protein Expr Purif*. 2012;82:380–388.
- [31] Santoro MM, Bolen DW. Unfolding free energy changes determined by the linear extrapolation



- method. 1. Unfolding of phenylmethanesulfonyl alpha-chymotrypsin using different denaturants. *Biochemistry*. 1988;27:8063–8068.
- [32] Pace CN. Determination and analysis of urea and guanidine hydrochloride denaturation curves. *Methods Enzymol*. 1986;131:266–280.
- [33] Swint L, Robertson AD. Thermodynamics of unfolding for turkey ovomucoid third domain: thermal and chemical denaturation. *Protein Sci*. 1993;2:2037–2049.
- [34] Fu H, Grimsley G, Scholtz JM, et al. Increasing protein stability: importance of  $\Delta C(p)$  and the denatured state. *Protein Sci*. 2010;19:1044–1052.